Adjustable Robust Nonlinear Network Design under Demand Uncertainties

Johannes Thürauf, Julia Grübel, Martin Schmidt

Abstract. We study network design problems for nonlinear and nonconvex flow models under demand uncertainties. To this end, we apply the concept of adjustable robust optimization to compute a network design that admits a feasible transport for all, possibly infinitely many, demand scenarios within a given uncertainty set. For solving the corresponding adjustable robust mixed-integer nonlinear optimization problem, we show that a given network design is robust feasible, i.e., it admits a feasible transport for all demand uncertainties, if and only if a finite number of worst-case demand scenarios can be routed through the network. We compute these worst-case scenarios by solving polynomially many nonlinear optimization problems. Embedding this result for robust feasibility in an adversarial approach leads to an exact algorithm that computes an optimal robust network design in a finite number of iterations. Since all of the results are valid for general potential-based flows, the approach can be applied to different utility networks such as gas, hydrogen, or water networks. We finally demonstrate the applicability of the method by computing robust gas networks that are protected from future demand fluctuations.

1. Introduction

Network design problems have been widely studied in the optimization literature due to their relevance in different applications such as transportation (Raghunathan 2013), telecommunication (Koster et al. 2013), or supply chains (Santoso et al. 2005). These problems typically involve optimizing a network design and the corresponding operation so that specific demand predictions are met and the overall costs are minimized. In most of the cases, these models contain uncertain parameters, which represent the deviation of the predictions from the actual demand in the future.

In this paper, we address these uncertainties for the class of mixed-integer nonlinear network design problems with demand uncertainties by using adjustable robust optimization (ARO). In a nutshell, the considered adjustable robust mixed-integer nonlinear optimization problem aims at minimizing the network expansion costs and has the following structure. We first decide on the so-called here-and-now decisions that represent the network expansion and have to be decided before the uncertain demand is known. Afterward, the uncertainty realizes in a worst-case manner within an a priori given uncertainty set. Finally, we have to guarantee that this worst-case scenario can be transported through the built network. Consequently, a solution of this problem yields a robust and resilient network, which is protected from all, possibly infinitely many, different demand fluctuations in the uncertainty set.

To model the physics of the network, we use nonlinear and nonconvex potential-based flows; see Gross et al. (2019). These flows are an extension of capacitated linear flows, which are typically used in network design problems. The main advantages of potential-based flows consist of their accurate representation of the underlying physics

Date: March 28, 2024.

2020 *Mathematics Subject Classification.* 90C11, 90C17, 90C35, 90C90.

Key words and phrases. Robust optimization, Nonlinear flows, Potential-based networks, Demand uncertainties, Mixed-integer nonlinear optimization.

and their broad applicability to model different types of utility networks such as gas, hydrogen, water, or lossless DC power flow networks. In the following, we particularly focus on the nonlinear and nonconvex cases. Thus, we aim to combine mixed-integer nonlinear optimization and robust optimization to compute resilient network designs while accurately considering the underlying physics and taking into account demand uncertainties.

Since the research on network design is rather extensive, we focus on the literature about robust network design and only start with a brief review regarding the works for nonlinear network design without uncertainties. Multiple approaches to solve nonlinear network design problems are based on different relaxations of the original problem. Raghunathan (2013) and Humpola and Fügenschuh (2015) develop different convex relaxations and embed the results in specific branch-and-bound frameworks to solve nonlinear network design problems. For the case of gas networks, Borraz-Sánchez et al. (2016) develop a mixed-integer second-order cone relaxation, which provides small gaps w.r.t. the optimal objective value of the corresponding mixed-integer nonlinear optimization problem (MINLP) in many cases. In the recent work by Li et al. (2024), the authors combine a convex reformulation and an efficient enumeration scheme to solve a specific gas network design problem. For a more detailed literature review on nonlinear network design without uncertainties, we refer to Li et al. (2024) for the case of gas networks and to D'Ambrosio et al. (2015) for the case of water networks.

A large part of the literature on robust network design with uncertain demand focuses on capacitated linear flow models. The approaches often distinguish between two different concepts of routing the flows. On the one hand, there are approaches that consider a so-called static routing. In this case, for each uncertain demand the corresponding flows have to follow a specific routing template, e.g., a linear function depending on the uncertain demand. This concept has been applied to robust network design problems with uncertain traffic (Koster et al. 2013; Ben-Ameur and Kerivin 2005). On the other hand, there are approaches using so-called dynamic routing, in which for each uncertain demand the flows can be chosen individually. Following this more general concept leads to an adjustable (or two-stage) robust mixed-integer linear network design problem; see, e.g., Atamtürk and Zhang (2007). These problems can be solved by specific branch-and-cut methods (Cacchiani et al. 2016) or by general methods of ARO; see Yanıkoğlu et al. (2019). A comparison of static and dynamic routing in addition to a so-called affine routing is discussed in Poss and Raack (2013).

We now turn to the considered case of adjustable robust network design for nonlinear flows, which is much less researched than the case of linear flows. For robust gas pipeline network expansion, Sundar et al. (2021) consider a box uncertainty set for the demand of sinks only. In this case, the authors show that two worst-case scenarios suffice to guarantee robust feasibility if there are no restrictions on the demand of the sources. For tree-shaped potential-based networks and a specific box uncertainty set for the demand of sinks and sources, Robinius et al. (2019) prove that polynomially many worst-case demand scenarios guarantee robust feasibility. To obtain these scenarios, the authors exploit the tree structure of the network and apply the obtained result to compute a robust diameter selection for hydrogen networks. A different notion of robustness of potential-based networks is investigated in Klimm et al. (2023), in which network topologies are characterized as robust if the maximal potential differences do not increase for decreasing demands. Moreover, Pfetsch and Schmitt (2023) compute robust potential-based networks, in which no demand uncertainties are considered, but the obtained robust network is protected from specific arc failures. For the related field of adjustable robust operation of potential-based networks, we refer to Aßmann et al.

(2019) as well as Kuchlbauer et al. (2022) and the references therein. Details about stochastic network design can be found in the recent work by Bertsimas et al. (2023).

In this paper, we develop an exact algorithm to solve an adjustable robust mixed-integer nonlinear network design problem with demand uncertainties. To this end, we focus on nonlinear and nonconvex potential-based flows and consider general demand uncertainty sets. Exploiting properties of potential-based flows and the underlying network, we show that adjustable robust feasibility of a given network expansion can be equivalently characterized by solving polynomially many optimization problems. These optimization problems consist of maximizing, respectively minimizing, specific network characteristics such as arc flows or potential differences w.r.t. the uncertainty set. Solving the latter problems leads to a finite set of worst-case demand scenarios, which prove adjustable robust feasibility or infeasibility of the considered network expansion. Embedding this characterization in an exact adversarial approach leads to an algorithm that solves the considered adjustable robust mixed-integer nonlinear optimization problem in a finite number of iterations. The algorithm starts with a small subset of demand scenarios that is iteratively augmented by worst-case demand scenarios obtained by the developed characterization of robust feasibility. We finally demonstrate the applicability of the developed approach by computing adjustable robust gas networks that are protected from future demand fluctuations. The numerical results show that only a small number of worst-case scenarios suffices to obtain an adjustable robust network design in practice.

The paper is organized as follows. In Section 2, we introduce potential-based flows and state the considered adjustable robust mixed-integer nonlinear network design problem under demand uncertainties. In Section 3, we derive an characterization of adjustable robust feasibility of a given network expansion based on finitely many worst-case demand scenarios. Subsequently, we embed this result in an exact adversarial approach that solves the uncertain network design problem. We present different solution techniques that speed up the performance of the developed approach in Section 4. Using an academic example, we then discuss that the number of necessary worst-case demand scenarios in the algorithm can significantly vary depending on the capacity of the sources; see Section 5. We finally demonstrate the applicability of the developed approach using the example of gas networks in Section 6, followed by a discussion of possible future research directions in Section 7.

2. Problem Statement

We now introduce the considered nonlinear potential-based flow model in Section 2.1 before we state the adjustable mixed-integer nonlinear network design problem in Section 2.2.

2.1. Potential-Based Networks.

We consider potential-based flows to model the underlying physical laws of the network flow. Potential-based flows form an extension of classic linear capacitated flow models and we now formally introduce them based on Gross et al. (2019) and Labbé et al. (2020). Let $G = (V, A)$ be a directed multi-graph consisting of a set of nodes V and a set of arcs A. The set of nodes V is partitioned into nodes V_+ at which flow is injected, nodes V_- at which flow is withdrawn, and inner nodes V_0 at which neither flow is injected nor withdrawn. Furthermore, the set A represents the arcs of the network and consists of triples (u, v, ℓ). Here, u and v represent the start and end node of the arc a and ℓ is the label of the arc. This modeling choice allows to consider multiple parallel arcs between two nodes, which often occurs in real-word utility networks.

In addition to the classic flow variables $q \in \mathbb{R}^A$, we consider nodal potential levels $\pi \in \mathbb{R}^V$. Due to technical restrictions, both the flow and the potential variables are bounded, i.e.,

$$\pi_u^- \le \pi_u \le \pi_u^+, \quad u \in V, \quad q_a^- \le q_a \le q_a^+, \quad a \in A.$$

To model the case of unbounded potentials or uncapacitated flows, we can set the potential bounds $\pi_u^- \le \pi_u^+, u \in V$, and the arc flow bounds $q_a^- \le q_a^+, a \in A$, to $\pm\infty$.

For a given arc $a \in A$, the incident potentials and the corresponding arc flow are coupled by a so-called potential function $\Phi_a \colon \mathbb{R} \to \mathbb{R}$. The potential function is usually nonlinear and nonconvex. We further assume that the properties

(i) Φ_a is continuous,
(ii) Φ_a is strictly increasing, and
(iii) Φ_a is odd, i.e., $\Phi_a(-x) = -\Phi_a(x)$,

hold, which are natural in the context of utility networks. The coupling between potentials and arc flows is given by

$$\pi_u - \pi_v = \Phi_a(q_a), \quad a = (u, v, \ell) \in A.$$

We further consider a demand vector $d \in \mathbb{R}^V_{\ge 0}$ that represents the injections and withdrawals at every node of the network. Hence, it holds $d_u = 0$ for each inner node $u \in V_0$. Since we consider stationary flows, this demand $d \in \mathbb{R}^V_{\ge 0}$ has to be balanced, i.e., the total amount of injections equals the total amount of withdrawals: $\sum_{u \in V_+} d_u = \sum_{u \in V_-} d_u$. We further have to impose mass flow conservation by

$$\sum_{a \in \delta^{\text{out}}(u)} q_a - \sum_{a \in \delta^{\text{in}}(u)} q_a = \begin{cases} d_u, & u \in V_+, \\ -d_u, & u \in V_-, \\ 0, & u \in V_0. \end{cases}$$

Combining the previous constraints leads to the formal definition of a potential-based flow.

Definition 1. *For a given demand $d \in \mathbb{R}^V_{\ge 0}$ with $d_u = 0$ for all $u \in V_0$, a tuple (q, π) is a feasible potential-based flow if and only if it satisfies*

$$\sum_{a \in \delta^{\text{out}}(u)} q_a - \sum_{a \in \delta^{\text{in}}(u)} q_a = \begin{cases} d_u, & u \in V_+, \\ -d_u, & u \in V_-, \\ 0, & u \in V_0, \end{cases}$$
$$\pi_u - \pi_v = \Phi_a(q_a), \quad a = (u, v, \ell) \in A,$$
$$\pi_u^- \le \pi_u \le \pi_u^+, \quad u \in V,$$
$$q_a^- \le q_a \le q_a^+, \quad a \in A.$$

One of the main advantages of using potential-based flows lies in their strong modeling capabilities w.r.t. flows in utility networks. In Gross et al. (2019), explicit potential functions for stationary gas (Φ^{G}), water (Φ^{W}), and lossless DC power-flow networks (Φ^{DC}) are presented. For an arc $a \in A$ and a corresponding arc flow q_a, these potential functions are explicitly given by

$$\Phi^{\text{G}}(q_a) = \Lambda_a q_a \left|q_a\right|, \quad \Phi^{\text{W}}(q_a) = \Lambda_a \operatorname{sgn}(q_a) \left|q_a\right|^{1.852}, \quad \Phi^{\text{DC}}(q_a) = \Lambda_a q_a, \tag{1}$$

where $\Lambda_a > 0$ is an arc specific constant depending on the application.

2.2. **Robust Network Design.** We now present an adjustable robust network expansion model that takes demand uncertainties into account. For modeling the underlying physics of the network flows, we use the potential-based flows as previously introduced.

In general, demand forecasts that are considered in the network design process are affected by uncertainties. Taking into account these demand uncertainties is of high relevance since even small perturbations of the injections and withdrawals can render the planned network design infeasible, i.e., the demand cannot be transported through the network. We now address these demand uncertainties by applying the well-established concept of (adjustable) robust optimization; see, Yanıkoğlu et al. (2019) and the references therein. To this end, we consider the demand uncertainty set

$$U := \left\{ d \in \mathbb{R}^V_{\geq 0} : \sum_{u \in V_+} d_u = \sum_{u \in V_-} d_u, \ d_u = 0, \ u \in V_0 \right\} \cap Z, \tag{2}$$

of balanced demands, where $Z \subset \mathbb{R}^V$ is a non-empty and compact set. We note that the general choice of the uncertainty set allows to consider convex, nonconvex, or discrete uncertainty sets.

With this uncertainty set at hand, the task of computing an adjustable robust network design consists of finding a cost-optimal network design such that for each demand uncertainty $d \in U$, there is a feasible transport through the built network.

For stating a corresponding adjustable robust optimization model, we partition the set of arcs A into existing arcs A_{ex} and into candidate arcs A_{ca} that can be built to enhance the capacity of the network. This allows to design a network from scratch ($A_{\text{ex}} = \emptyset$) as well as to increase the capacity of existing networks ($A_{\text{ex}} \neq \emptyset$). We further introduce binary variables $x \in X \subseteq \{0,1\}^{A_{\text{ca}}}$. Here, for an arc $a \in A_{\text{ca}}$, the binary variable x_a equals one if the candidate arc a is built and otherwise, it is zero. Further, expanding the network by an arc $a \in A_{\text{ca}}$ results in costs $c_a > 0$. The set X can contain additional constraints on the expansion decisions such as that only one out of multiple parallel arcs in A_{ca} can be built. The latter occurs in the discrete selection of pipeline diameters in gas networks; see, e.g., Li et al. (2024). We are now ready to state a model that computes an adjustable robust network design that guarantees that each demand scenario in the uncertainty set U can be transported:

$$\nu(U) := \min_{x,q,\pi} \quad \sum_{a \in A_{\text{ca}}} c_a x_a \tag{3a}$$

$$\text{s.t.} \quad x \in X, \tag{3b}$$

$$\forall d \in U \, \exists \left(q^d, \pi^d\right) \ \text{with} \tag{3c}$$

$$\sum_{a \in \delta^{\text{out}}(u)} q_a^d - \sum_{a \in \delta^{\text{in}}(u)} q_a^d = \begin{cases} d_u, & u \in V_+, \\ -d_u, & u \in V_-, \\ 0, & u \in V_0, \end{cases} \tag{3d}$$

$$\pi_u^d - \pi_v^d = \Phi_a(q_a^d), \quad a = (u,v,\ell) \in A_{\text{ex}}, \tag{3e}$$

$$\pi_u^d - \pi_v^d \leq \Phi_a(q_a^d) + (1 - x_a) M_a^+, \quad a = (u,v,\ell) \in A_{\text{ca}}, \tag{3f}$$

$$\pi_u^d - \pi_v^d \geq \Phi_a(q_a^d) + (1 - x_a) M_a^-, \quad a = (u,v,\ell) \in A_{\text{ca}}, \tag{3g}$$

$$q_a^- \leq q_a^d \leq q_a^+, \quad a \in A_{\text{ex}}, \tag{3h}$$

$$q_a^- x_a \leq q_a^d \leq q_a^+ x_a, \quad a \in A_{\text{ca}}, \tag{3i}$$

$$\pi_u^- \leq \pi_u^d \leq \pi_u^+, \quad u \in V. \tag{3j}$$

In the objective function (3a), we minimize the costs associated to the chosen network design. Constraints (3b) impose additional restrictions on the network design. Then, for every demand uncertainty $d \in U$, we determine flows q^d and potentials π^d such that mass flow conservation (3d) and the potential bounds (3j) are satisfied. Furthermore, we ensure by Constraints (3e)–(3g) that the coupling between the potentials and the arc flows is satisfied for all existing arcs and all candidate arcs that are built. Moreover, we guarantee that for existing and new arcs specific flow capacities are satisfied. If a candidate arc $a \in A_{\text{ca}}$ is not built, i.e., $x_a = 0$, then the corresponding arc flow is set to zero; see Constraints (3i).

In line with Schmidt and Thürauf (2022), we now discuss that for each arc (u, v, ℓ), the big-M values

$$M_a^+ = \pi_u^+ - \pi_v^-, \quad M_a^- = \pi_u^- - \pi_v^+, \tag{4}$$

are valid. Here, valid means that if a candidate arc $a = (u, v, \ell) \in A_{\text{ca}}$ is not built, i.e., $x_a = 0$, the Constraints (3f) and (3g) are redundant and we have no coupling between the incident potentials and the corresponding arc flow. To see this, let us consider a candidate arc $a \in A_{\text{ca}}$ with $x_a = 0$ and an arbitrary uncertain demand $d \in U$. Then, from Constraints (3i), it follows $q_a^d = 0$. Consequently, from Constraints (3j) and $\Phi_a(0) = 0$, we obtain $M_a^- = \pi_u^- - \pi_v^+ \leq \pi_u^d - \pi_v^d \leq \pi_u^+ - \pi_v^- = M_a^+$, which corresponds to Constraints (3f) and (3g).

From the perspective of robust optimization, Problem (3) is an adjustable robust optimization problem. The expansion variables x represent the first-stage or so-called "here-and-now" decisions and the flows q^d as well as the potentials π^d are second-stage or so-called "wait-and-see" decisions, which are adapted for each uncertainty $d \in U$.

Remark 1. *For linear potential functions Φ_a, Problem (3) is an adjustable robust mixed-integer linear optimization problem that can be tackled by standard methods of adjustable linear robust optimization, e.g., by methods based on column-and-constraint generation; see Zhao and Zeng (2012) and Lefebvre et al. (2022).*

In the light of this remark, we now focus on nonlinear and nonconvex potential functions Φ_a, which occur, e.g., in gas, hydrogen, or water networks; see (1). Thus, we obtain an adjustable robust mixed-integer nonlinear optimization problem (3), for which the set of applicable methods of the literature is scarce.

3. Exact Adversarial Approach

We now follow the idea of the well-known adversarial approach in robust optimization (Bienstock and Özbay 2008), to solve Problem (3) to global optimality. The main idea of the adversarial approach is to replace the original uncertainty set U by a finite set $S \subseteq U$ of "worst-case" scenarios. To this end, the approach starts with a small set of scenarios S and then solves Problem (3) w.r.t. S instead of U. The latter problem is now a mixed-integer nonlinear optimization problem consisting of finitely many variables and constraints due to $|S| < \infty$. If the obtained solution is robust feasible, i.e., it is feasible for the original problem w.r.t. U, then it is also optimal due to $S \subseteq U$. Otherwise, there are scenarios $U \setminus S$ that render the obtained point infeasible. If this is the case, at least one of these scenarios is added to S and the procedure repeats by solving the robust problem w.r.t. the updated S. When applying the adversarial approach, the most important questions to answer are:

(i) How to verify that a given point is robust feasible?
(ii) How to compute a scenario in $U \setminus S$ that certifies the infeasibility of a given point?
(iii) Does the adversarial approach terminate after a finite number of steps?

For strict robust optimization, Questions (i) and (ii) are usually addressed by maximizing the constraint violation w.r.t. the uncertainty set and a fixed "here-and-now" decision. Furthermore, for linear constraints and polyhedral uncertainty sets, the method terminates after a finite number of steps; see Bertsimas et al. (2016).

However, for the considered case of ARO, applying the adversarial approach is even more challenging since we cannot directly transfer the idea to compute a violating scenario of the strictly robust case to the adjustable robust one. This is mainly based on the fact that in ARO, we can determine the second-stage decisions after the uncertainty realizes.

For adjustable robust linear problems with polyhedral uncertainty sets, it is shown that adding finitely many "worst-case" scenarios suffices; see Ayoub and Poss (2016). An analogous result is shown for adjustable robust nonconvex optimization with uncertainty sets being polytopes under specific quasi-convexity assumptions; see Takeda et al. (2008). However, for the considered adjustable robust mixed-integer nonlinear problem and the general choice of uncertainty set (2), these approaches cannot be directly applied.

We now exploit structural properties of potential-based flows and the underlying graph to answer Questions (i)–(iii) for the considered Problem (3). In particular, we show that for given first-stage decisions $x \in X$, we can verify robust feasibility, respectively compute a violating scenario, by solving polynomially (in the encoding-length of the underlying graph) many single-level nonlinear optimization problems. To this end, we start with the case of weakly connected graphs and then extend these results to general graphs. For a given expansion decision $x \in X$, we now consider three different classes of nonlinear optimization problems. Solving these "adversarial" problems either verifies robust feasibility of x or yields a demand scenario $d \in U$ that certifies the infeasibility of x.

First, for a given pair of nodes $(u, v) \in V^2$, we compute the maximum potential difference between u and v within the uncertainty set U by

$$\varphi_{u,v}(x) := \max_{d,q,\pi} \ \pi_u - \pi_v \quad \text{s.t.} \quad \text{(3d)–(3g)}, \ d \in U. \tag{5}$$

In Problem (5), we explicitly dismiss the flow and potential bounds (3h)–(3j). The intuition behind this is to compute scenarios that induce the most stress on the network w.r.t. the potential levels, i.e., we are particularly interested in scenarios that violate the potential bounds. For the given expansion decision x, we will later show that we can only find feasible second-stage decisions π if and only if the objective value of Problem (5) stays below specific bounds. Thus, solving Problem (5) for each pair of nodes leads to finitely many "worst-case" scenarios regarding the potential levels π and the given expansion decision x. We note that these worst-case scenarios are also considered in, e.g., Labbé et al. (2020), Aßmann et al. (2019), and Robinius et al. (2019) in the context of gas market problems, of robust control of gas networks, and of robust selection of diameters in tree-shaped networks. Moreover, solving Problem (5) can be done in polynomial time for box uncertainty sets and tree-shaped networks (Robinius et al. 2019). However, it is NP-hard for general potential-based flows in general graphs; see Thürauf (2022).

Second and third, we compute for each arc $a \in A$ the minimum and maximum arc flow within the considered uncertainty set U by

$$\underline{q}_a(x) := \min_{d,q,\pi} \ q_a \quad \text{s.t.} \quad \text{(3d)–(3g)}, \ d \in U \tag{6}$$

and

$$\bar{q}_a(x) := \max_{d,q,\pi} \ q_a \quad \text{s.t.} \quad \text{(3d)–(3g)}, \ d \in U. \tag{7}$$

We again dismiss potential and flow bounds in Problems (6) and (7) because we are particularly interested in finding scenarios that violate the flow bounds. Analogously, we will show that for the given expansion decision x, we can only find feasible second-stage decisions q if and only if the objective values of (6) and (7) satisfy specific bounds. Thus, solving these problems leads to a finite set of "worst-case" scenarios regarding the flows.

We now prove that we can verify robust feasibility of given first-stage decisions $x \in X$ by solving the polynomially many Problems (5)–(7). To this end, we use the following auxiliary lemma from the literature, which states that for a given demand the corresponding flows and potential differences are unique.

Lemma 1. *Let $x \in X$ be fixed and let $G'(x) = (V, A_{\text{ex}} \cup \{a \in A_{\text{ca}} : x_a = 1\})$ be the expanded graph. Further, we assume that $G'(x)$ is weakly connected. For a fixed* *demand $d \in U$, there are potentials π' and unique flows q such that the set of feasible points that satisfies Constraints (3d)–(3g) and $q_a = 0$ for each arc $a \in \{\tilde{a} \in A_{\text{ca}} : x_{\tilde{a}} = 0\}$ is non-empty and given by*

$$\{(q, \pi) : \pi = \pi' + \mathbb{1}\eta,\ \eta \in \mathbb{R}\}$$

where $\mathbb{1}$ is a vector of ones in appropriate dimension.

Proof. The lemma follows from Theorem 7.1 of Humpola et al. (2015) and the fact that for every arc a with $x_a = 0$, the corresponding flows are zero. □

We now characterize robust feasibility of given expansion decisions $x \in X$ using Problems (5)–(7) for the case of a weakly connected expanded graph.

Theorem 1. *Let $x \in X$ be fixed and let $G'(x) = (V, A'(x))$ be the expanded graph, i.e., $A'(x) := A_{\text{ex}} \cup \{a \in A_{\text{ca}} : x_a = 1\}$. Further, we assume that $G'(x)$ is weakly connected. Then, Constraints (3c)–(3j) are satisfied w.r.t. x if and only if for every pair of nodes $(u, v) \in V^2$, the corresponding maximum potential difference satisfies the potential bounds*

$$\varphi_{u,v}(x) \le \pi_u^+ - \pi_v^- \tag{8}$$

and for each arc $a \in A'(x)$, the minimum and maximum arc flow satisfies the corresponding flow bounds, i.e.,

$$\underline{q}_a(x) \ge q_a^- \quad \text{and} \quad \bar{q}_a(x) \le q_a^+. \tag{9}$$

Proof. For a fixed expansion $x \in X$, let Constraints (3c)–(3j) be satisfied. We now distinguish two cases. First, we assume for the sake of contradiction that an arc $a \in A'(x)$ exists such that $\underline{q}_a(x) < q_a^-$ holds. Let (d, q, π) be a corresponding optimal solution of (6). Applying Lemma 1 to demand d shows that there are unique flows q satisfying Constraints (3d)–(3g) and $q_a = 0$ for each arc $a \in \{\tilde{a} \in A_{\text{ca}} : x_{\tilde{a}} = 0\}$. Due to the feasibility of Constraints (3c)–(3j) w.r.t. x, these flows satisfy Constraints (3h) and (3i). This contradicts the assumption $\underline{q}_a(x) < q_a^-$. Thus, $\underline{q}_a(x) \ge q_a^-$ is true for each $a \in A'(x)$. The case of the upper flow bound can be handled analogously. Consequently, Conditions (9) hold.

Second, we now assume for the sake of contradiction that there is a pair of nodes $(u, v) \in V^2$ such that $\varphi_{u,v}(x) > \pi_u^+ - \pi_v^-$. Let (d, q, π) be a corresponding optimal solution of (5). Due to Lemma 1 and the feasibility of Constraints (3c)–(3j) w.r.t. x, there is a point (d, q, π') that is feasible for Constraints (3d)–(3j) and that satisfies $q_a = 0$ for each arc $a \in \{\tilde{a} \in A_{\text{ca}} : x_{\tilde{a}} = 0\}$. The potential bounds (3j) imply $\pi'_u - \pi'_v \le \pi_u^+ - \pi_v^-$. From Lemma 1, it follows that there is an $\eta \in \mathbb{R}$ so that $\pi' + \mathbb{1}\eta = \pi$ holds. Consequently, we obtain the contradiction

$$\pi_u^+ - \pi_v^- \ge \pi'_u - \pi'_v = \pi'_u + \eta - (\pi'_v + \eta) = \pi_u - \pi_v = \varphi_{u,v}(x).$$

We now examine the reverse direction. Thus, for fixed expansion $x \in X$, Conditions (8) and (9) are satisfied. Let $d \in U$ be an arbitrary demand. Due to Lemma 1, there is a feasible point (d, q, π) that satisfies Constraints (3d)–(3g) and $q_a = 0$ for each arc $a \in \{\tilde{a} \in A_{\text{ca}} : x_{\tilde{a}} = 0\}$. In addition, Lemma 1 implies that we can shift the potentials so that $\pi_u \le \pi_u^+$ for every node $u \in V$ holds and there is a node w with $\pi_w = \pi_w^+$. This point (d, q, π) is feasible for Problems (6) and (7) since no arc flow or potential bounds are present in these problems. Consequently, from Condition (9), it follows that the flow bounds (3h) and (3i) are satisfied.

We now assume for the sake of contradiction that there is a node $h \in V$ with $\pi_h < \pi_h^-$. Then, it follows

$$\pi_w - \pi_h = \pi_w^+ - \pi_h > \pi_w^+ - \pi_h^-,$$

which is a contradiction to Condition (8) since (d, q, π) is a feasible point for Problem (5) w.r.t. the pair of nodes (w, h). Consequently, for every node $u \in V$, $\pi_u \geq \pi_u^-$ is satisfied. We note that the potentials satisfy the upper potential bounds due to the specific choice of the considered point (d, q, π). Hence, Constraints (3j) are also satisfied and the point (d, q, π) is feasible for Constraints (3d)–(3j). Since d is an arbitrary demand in U, this concludes the proof. □

We now extend the obtained characterization of robust feasibility to the case that the expansion decision $x \in X$ leads to an expanded graph $G'(x)$ that has at least two connected components. To this end, for a given connected component $G^i = (V^i, A^i)$[1], we consider another auxiliary problem for computing the maximal absolute flow that has to be transported between the connected component G^i and the remaining network in the uncertainty set. This problem reads

$$\mu_{G^i}(x) := \max_{d} |y| \quad \text{s.t.} \quad y = \sum_{u \in V^i \cap V_+} d_u - \sum_{u \in V^i \cap V_-} d_u, \ d \in U. \tag{10}$$

The value $\mu_{G^i}(x)$ is positive if and only if there is a scenario $d \in U$ with excess demand or excess supply regarding the connected component G^i. In this case, $\mu_{G^i}(x) > 0$, the expansion decision $x \in X$ is robust infeasible.

Lemma 2. *Let $x \in X$ be fixed and $G'(x) = (V, A_{\text{ex}} \cup \{a \in A_{\text{ca}} : x_a = 1\})$ be the expanded graph. Furthermore, let $\mathcal{G}'(x) := \{G^1, \dots, G^n\}$ with $G^i = (V^i, A^i)$ be the set of connected components of the expanded graph $G'(x)$. Then, Constraints (3c)–(3j) can only be satisfied w.r.t. x if for every connected component G^i with $i \in \{1, \dots, n\}$ of the expanded network $G'(x)$, the maximum excess demand or excess supply is zero, i.e., $\mu_{G^i}(x) = 0$.*

Proof. If there is a connected component G^i with $i \in \{1, \dots, n\}$ so that $\mu_{G^i}(x) > 0$ holds, then there is a scenario $d \in U$ such that there is excess demand or excess supply in G^i. Consequently, this scenario cannot be transported through the network since mass flow conservation (3d) cannot be satisfied in the connected component G^i. □

We note that if the graph consists only of a single connected component, then it directly follows that the optimal objective value of Problem (10) is zero because we only consider balanced demands in the uncertainty set (2). Using the previous lemma, we now extend Theorem 1 to the case of multiple connected components in the expanded graph.

Theorem 2. *Let $x \in X$ be fixed and $G'(x) = (V, A_{\text{ex}} \cup \{a \in A_{\text{ca}} : x_a = 1\})$ be the expanded graph. Furthermore, let $\mathcal{G}'(x) := \{G^1, \dots, G^n\}$ with $G^i = (V^i, A^i)$ be the set of connected components of the expanded graph $G'(x)$. Then, Constraints (3c)–(3j) are satisfied w.r.t. x if and only if*

$$\mu_{G^i}(x) = 0 \quad \text{for all } G^i \in \mathcal{G}'(x), \tag{11a}$$

$$\varphi_{u,v}(x) \leq \pi_u^+ - \pi_v^- \quad \text{for all } (u, v) \in (V^i)^2, \ G^i \in \mathcal{G}'(x), \tag{11b}$$

$$\underline{q}_a(x) \geq q_a^- \quad \text{for all } a \in A^i, \ G^i \in \mathcal{G}'(x), \tag{11c}$$

$$\bar{q}_a(x) \leq q_a^+ \quad \text{for all } a \in A^i, \ G^i \in \mathcal{G}'(x), \tag{11d}$$

holds.

Proof. For a given expansion $x \in X$, let the Constraints (3c)–(3j) be satisfied. Then, from Lemma 2, it follows that Condition (11a) holds. Hence, every $d \in U$ is balanced w.r.t. each connected component, i.e., $\sum_{u \in V_+ \cap V^i} d_u = \sum_{u \in V_- \cap V^i} d_u$ for each $i \in \{1, \dots, n\}$.

[1]For the ease of presentation, we write $G^i = (V^i, A^i)$ instead of $G^i(x) = (V^i(x), A^i(x))$ in the following.

Consequently, we can apply Theorem 1 to each connected component G^i while using as uncertainty set the original uncertainty set projected onto the nodes V^i of the connected component. This proves that Conditions (11) are satisfied.

For fixed expansion $x \in X$, we now assume that Conditions (11) hold. Since Conditions (11a) are satisfied, every $d \in U$ is balanced w.r.t. each connected component. Consequently, for each connected component, we can apply Lemma 1. Thus, for each demand $d \in U$, there are potentials π' and unique flows q such that the set of feasible points satisfying Constraints (3d)–(3g) w.r.t. x and $q_a = 0$ for each arc $a \in \{\tilde{a} \in A_{\text{ca}} : x_{\tilde{a}} = 0\}$ is non-empty and given by

$$\{(q, \pi) : (\pi_u)_{u \in V^i} = (\pi'_u + \eta_i)_{u \in V^i}, \ \eta_i \in \mathbb{R}, \ i \in |\mathcal{G}'(x)|\}.$$

Using this statement, we can apply the second part of the proof of Theorem 1 to every connected component G^i, which proves the claim. □

For a given expansion decision, Theorem 2 allows to verify robust feasibility by solving at most $|V| + |V|^2 + 2|A|$ many nonlinear optimization problems. Furthermore, in case of robust infeasibility of the expansion decision, solving these problems provides violating scenarios in U that render the expansion decision infeasible. Consequently, Theorem 2 resolves the main challenges (i) and (ii) when applying the adversarial approach to the considered adjustable robust mixed-integer nonlinear optimization problem (3). We note that for checking robust feasibility, we have to solve the nonconvex adversarial problems to global optimality. In doing so, also the specific choice of the potential-based flow model as well as the choice of the uncertainty set influence the computational complexity of this task. However, in the conducted computational study the adversarial problems are solved rather fast and the MINLPs (3) pose a much bigger computational challenge.

Embedding the results of Theorem 2 into the adversarial approach leads to Algorithm 1. We note that there are multiple possibilities on how to integrate the characterization of robust feasibility of Theorem 2 in an adversarial approach. In our implementation of Algorithm 1, we aim to keep the size of the MINLP (3) w.r.t. S as small as possible since solving this MINLP is computationally challenging. Since the size of this problem increases with the size of the scenario set S, for an infeasible expansion decision, we only add a single violating scenario to cut off this robust infeasible point. More precisely, we first solve the adversarial problems (10) since these problems are typically less challenging than Problems (5)–(7), which contain the constraints of the nonconvex potential-based flows. If solving Problems (10) leads to violating scenarios, i.e., $\mu_{G^i}(x) > 0$ holds, then we add this scenario to cut off the robust infeasible expansion decision x and start a new iteration. Otherwise, we solve the adversarial problems (5), respectively (6) and (7), and add a most violating scenario to the set of demands S if applicable. In general, it is also possible to stop solving these adversarial problems after a first violating scenario is computed as for the case of Problems (10). However, preliminary computational results showed that adding a most violating scenario w.r.t. (5) leads to a lower number of iterations of the algorithm. We finally note that all adversarial problems (10) and (5)–(7) can also be solved in parallel since they do not depend on each other.

We conclude this section with a positive answer for the main challenge (iii).

Theorem 3. *Algorithm 1 terminates after a finite number of iterations and either returns an adjustable robust solution of Problem* (3) *or proves its infeasibility.*

Proof. If we consider a robust infeasible expansion decision $x \in X$, i.e., it cannot be extended to satisfy Constraints (3c)–(3j) for all $d \in U$, then there exists a demand $d \in U$ that violates one of the conditions in (11). Due to the construction of the algorithm, one of these violating demands is added to the set of scenarios S if x is part of the optimal solution in Line 2. Consequently, the considered network expansion $x \in X$ is excluded in

Algorithm 1: Adversarial approach to solve the network design problem (3)

Input: A Graph $G = (V, A_{\text{ex}} \cup A_{\text{ca}})$ and an uncertainty set U satisfying (2).
Output: An optimal adjustable robust expansion $x \in X$ for Problem (3) or an indication of infeasibility.

1 Determine a finite set of scenarios $S \subseteq U$.
2 Solve Problem (3) w.r.t. S (instead of U) to get (x, q, π).
3 **if** *the problem is infeasible* **then**
4   **return** The problem is infeasible.
5 Determine the set of all connected components $\mathcal{G}'(x)$ of the expanded graph $G'(x) = (V, A_{\text{ex}} \cup \{a \in A_{\text{ca}} : x_a = 1\})$.
6 **for** $G^i \in \mathcal{G}'(x)$ **do**
7   Solve Problem (10) to get d' with objective value $\mu_{G^i}(x)$.
8   **if** $\mu_{G^i}(x) > 0$ **then**
9         $S = S \cup \{d'\}$ and go to Line 2.
10 Set $\varphi^{\max} = 0$.
11 **for** $G^i \in \mathcal{G}'(x)$ **do**
12   **for** $(u, v) \in (V^i)^2$ **do**
13   Solve Problem (5) w.r.t. G^i to get (d', q', π') with objective value $\varphi_{u,v}(x)$.
14   **if** $\varphi_{u,v}(x) > \pi_u^+ - \pi_v^-$ *and* $\varphi_{u,v}(x) - (\pi_u^+ - \pi_v^-) > \varphi^{\max}$ **then**
15   Set $\varphi^{\max} = \varphi_{u,v}(x) - (\pi_u^+ - \pi_v^-)$ and $d^{\max} = d'$.
16 **if** $\varphi^{\max} > 0$ **then**
17     $S = S \cup \{d^{\max}\}$ and go to Line 2.
18 Set $q^{\max} = 0$.
19 **for** $G^i \in \mathcal{G}'(x)$ **do**
20   **for** $a \in A^i$ **do**
21   Solve Problem (6) w.r.t. G^i to get (d', q', π') with objective value $\underline{q}_a(x)$.
22   **if** $\underline{q}_a(x) < q_a^-$ *and* $q_a^- - \underline{q}_a(x) > q^{\max}$ **then**
23   Set $q^{\max} = q_a^- - \underline{q}_a(x)$ and $d^{\max} = d'$.
24   Solve Problem (7) w.r.t. G^i to get (d', q', π') with objective value $\bar{q}_a(x)$.
25   **if** $\bar{q}_a(x) > q_a^+$ *and* $\bar{q}_a(x) - q_a^+ > q^{\max}$ **then**
26   Set $q^{\max} = \bar{q}_a(x) - q_a^+$ and $d^{\max} = d'$.
27 **if** $q^{\max} > 0$ **then**
28     $S = S \cup \{d^{\max}\}$ and go to Line 2.
29 **return** Optimal adjustable robust network design $x \in X$.

the next iteration. Thus, the algorithm terminates after a finite number of iterations because we only have a finite number of possible assignments for $x \in X \subseteq \{0,1\}^{|A_{\text{ca}}|}$. Since Problem (3) w.r.t. S is a relaxation of Problem (3) w.r.t. U, the algorithm either correctly returns an optimal solution or correctly verifies infeasibility. □

4. Enhanced Solution Techniques

When applying Algorithm 1, there are two main challenges from the computational point of view. For verifying robust feasibility, the adversarial problems (5)–(7) have to be solved to global optimality. In particular, solving $|V|^2$ many problems (5) can be computationally expensive. In addition, solving the MINLP (3) w.r.t. the worst-case scenarios S becomes more demanding from iteration to iteration due to the increasing set of scenarios S. In the following, we present different techniques that address these computational challenges.

4.1. **Reducing the Number of Adversarial Problems.** We now prove that under specific assumptions on the potential bounds, we can significantly reduce the number of adversarial problems (5) that have to be solved to verify robust feasibility. The intuition is based on the observation that in the considered potential-based flow setting, there is always a source node with maximal potential level and a sink node with minimal potential level.

Observation 4. *Let $x \in X$ be fixed and let $G^i = (V^i, A^i)$ be a connected component of the expanded graph $G'(x) = (V, A_{\text{ex}} \cup \{a \in A_{\text{ca}} : x_a = 1\})$. Further, let the point (d, q, π) satisfy Constraints (3d)–(3g) w.r.t. G^i. Then, there is a source node $w \in V^i_+ := V_+ \cap V^i$ with $\pi_w = \max_{v \in V^i} \pi_v$ and a sink node $u \in V^i_- := V_- \cap V^i$ with $\pi_u = \min_{v \in V^i} \pi_v$.*

This observation follows from the assumption that for every arc $a \in A$, the potential function Φ_a is strictly increasing. Consequently, sending flow from a source to a sink node leads to a positive potential drop. Using this observation, we now prove that under specific requirements for the potential bounds, we only have to compute the maximum potential difference, i.e., solve Problem (5), between sources and sinks.

Lemma 3. *Let $x \in X$ be fixed and let $G^i = (V^i, A^i)$ be a connected component of the expanded graph $G'(x) = (V, A_{\text{ex}} \cup \{a \in A_{\text{ca}} : x_a = 1\})$. For each source $w \in V^i_+ := V_+ \cap V^i$, let the upper potential bound satisfy $\pi^+_w \leq \pi^+_v$ for all sinks and inner nodes $v \in (V_- \cup V_0) \cap V^i$. For each sink $u \in V^i_- := V_- \cap V^i$, let the lower potential bound satisfy $\pi^-_u \geq \pi^-_v$ for all sources and inner nodes $v \in (V_+ \cup V_0) \cap V^i$. Then,*

$$\varphi_{u,v}(x) \leq \pi^+_u - \pi^-_v \quad \text{for all } (u, v) \in V^i_+ \times V^i_- \tag{12}$$

implies

$$\varphi_{u,v}(x) \leq \pi^+_u - \pi^-_v \quad \text{for all } (u, v) \in (V^i)^2.$$

Proof. Let the inequalities in (12) be satisfied. We now contrarily assume that there is a node pair $(m, n) \in (V^i)^2 \setminus V^i_+ \times V^i_-$ that satisfies $\varphi_{m,n}(x) > \pi^+_m - \pi^-_n$. Hence, there exists a solution (d, q, π) of Problem (5) with $\pi_m - \pi_n > \pi^+_m - \pi^-_n$. From Observation 4, it follows that there is a source $w \in V^i_+$ with $\pi_w = \max_{v \in V^i} \pi_v$ and a sink $u \in V^i_-$ with $\pi_u = \min_{v \in V^i} \pi_v$. We now conduct a case distinction.

If $m \in (V_- \cup V_0) \cap V^i$ and $n \in (V_+ \cup V_0) \cap V^i$, we obtain the contradiction

$$\varphi_{m,n}(x) = \pi_m - \pi_n \leq \pi_w - \pi_u \leq \varphi_{w,u}(x) \leq \pi^+_w - \pi^-_u \leq \pi^+_m - \pi^-_n,$$

where the last inequality follows from the assumptions on the potential bounds. Additionally, if $m \in (V_- \cup V_0) \cap V^i$ and $n \in V^i_-$, we obtain the contradiction

$$\varphi_{m,n}(x) = \pi_m - \pi_n \leq \pi_w - \pi_n \leq \varphi_{w,n}(x) \leq \pi^+_w - \pi^-_n \leq \pi^+_m - \pi^-_n.$$

Finally, if $m \in V^i_+$ and $n \in (V_+ \cup V_0) \cap V^i$, then we obtain the contradiction

$$\varphi_{m,n}(x) = \pi_m - \pi_n \leq \pi_m - \pi_u \leq \varphi_{m,u}(x) \leq \pi^+_m - \pi^-_u \leq \pi^+_m - \pi^-_n. \qquad \square$$

As a consequence of this lemma, we can reduce the maximal number of adversarial problems (5) that have to be solved to check robust feasibility from $|V|^2$ to at most $|V_+| \times |V_-|$ many problems. In the case of real-world utility networks, this reduction is significant because usually there are only a small number of sources in these networks. Furthermore, the assumptions regarding the potential bounds are often satisfied in utility networks such as gas or water networks.

We additionally remark that we can add to the adversarial problems (5) w.r.t. (u, v) the constraint

$$\pi_u - \pi_v \geq \pi_u^+ - \pi_v^- .$$

If this constraint renders the adversarial problem infeasible, then we can directly conclude that there is no violating scenario w.r.t. (u, v). Preliminary computational results have shown that this approach significantly speeds up the computational process. Analogously, we can add the constraints $q_a \leq q_a^-$ to Problem (6) and $q_a \geq q_a^+$ to Problem (7).

4.2. **Computing Lower Bounds.** We now focus on the algorithmic idea to iteratively update a lower bound for the objective function of the MINLP (3) w.r.t. S by exploiting the structure of Algorithm 1. Thus, we add to the MINLP (3) the constraint

$$\sum_{a \in A_{\text{ca}}} c_a x_a \geq \kappa, \tag{13}$$

where $\kappa \in \mathbb{R}_{\geq 0}$ is a valid lower bound of the objective value of Problem (3) that we iteratively update. Here, "valid" means that we do not cut off any optimal solution by adding Constraint (13).

Since we increase the set of scenarios S in each iteration of Algorithm 1, we can use the optimal objective value of Problem (3) of the previous iteration, i.e., without the last added "worst-case" scenario d', as a lower bound for the optimal objective value in the next iteration. Thus, we can iteratively set $\kappa = \nu(S \setminus \{d'\})$, where $\nu(S \setminus \{d'\})$ is the optimal objective value of Problem (3) w.r.t. the scenario set $S \setminus \{d'\}$. We note that obtaining this lower bound is straightforward and computationally cheap since we already solved the corresponding MINLPs in Algorithm 1. However, this bound can be improved since it dismisses all information regarding the last added worst-case scenario d'. To do so, we now present two relaxations of the MINLP (3) that can be solved prior to solving Problem (3) to improve the lower objective bound κ.

First, we can solve the MINLP (3) only w.r.t. the last added "worst-case" scenario d', which is a relaxation of Problem (3) due to $\{d'\} \subseteq S$. The benefit of this simple relaxation is that the size of the corresponding MINLP, i.e., the number of variables and constraints, does not increase from iteration to iteration, in contrast to Problem (3) w.r.t. the entire set S. In the following, we denote this relaxation as Reduced Relaxation. Our computational results of Section 6.4 indicate that this relaxation is particularly useful at the early iterations in Algorithm 1.

Second, we apply a well-known mixed-integer second-order cone relaxation for gas networks, see Borraz-Sánchez et al. (2016), to the considered general potential-based flows. This relaxation leads to a mixed-integer convex problem if for each arc $a \in A$, the potential functions Φ_a are convex on the domain $\mathbb{R}_{\geq 0}$. This is the case, e.g., for water and gas networks; see (1). In line with Borraz-Sánchez et al. (2016), we start with an equivalent reformulation of the Constraints (3e)–(3g) using additional binary variables that indicate the flow direction. To this end, for each arc $a = (u, v, \ell) \in A$ and demand $d \in U$, we introduce a binary variable $y_a^d \in \{0, 1\}$. The binary variable equals one if the flow is from node u to node v and otherwise, it is zero. This is ensured by the constraints

$$q_a^- (1 - y_a^d) \leq q_a^d \leq q_a^+ y_a^d, \quad a \in A, \tag{14}$$

where q^d are the corresponding flows of Problem (3). We note that for an arc flow of zero, i.e., $q_a^d = 0$, the variable y_a^d can be chosen arbitrarily. Moreover, we assume that for each arc $a \in A$, the flow bounds satisfy $q_a^- \leq 0 \leq q_a^+$, which is a natural assumption in the context of potential-based flows. Using the introduced binary variables for the flow directions and the symmetry of the potential functions, i.e., $\Phi_a(-q_a^d) = -\Phi_a^d(q_a^d)$, we can equivalently[2] reformulate Constraints (3e)–(3g) as

$$(\pi_v^d - \pi_u^d) + 2y_a^d(\pi_u^d - \pi_v^d) = \Phi_a(|q_a^d|), \quad a = (u,v,\ell) \in A_{\text{ex}}, \tag{15a}$$

$$(\pi_v^d - \pi_u^d) + 2y_a^d(\pi_u^d - \pi_v^d) \le \Phi_a(|q_a^d|) + (1 - x_a)M_a^+, \quad a = (u,v,\ell) \in A_{\text{ca}}, \tag{15b}$$

$$(\pi_v^d - \pi_u^d) + 2y_a^d(\pi_u^d - \pi_v^d) \ge \Phi_a(|q_a^d|) + (1 - x_a)M_a^-, \quad a = (u,v,\ell) \in A_{\text{ca}}. \tag{15c}$$

Analogously to (4), for each arc $a = (u,v,\ell) \in A_{\text{ca}}$, we adapt the big-$M$ values to $M_a^+ = \max\{\pi_u^+ - \pi_v^-, \pi_v^+ - \pi_u^-\}$ and $M_a^- = \min\{\pi_u^- - \pi_v^+, \pi_v^- - \pi_u^+\}$. We note that the bilinear terms on the left-hand side of Constraints (15) can be linearized using the inequalities of McCormick (1976); see Appendix A for the corresponding reformulations. Using these constraints we can equivalently represent the expansion problem (3) by the MINLP

$$\nu(U) := \min_{x,q,\pi} \sum_{a \in A_{\text{ca}}} c_a x_a \quad \text{s.t.} \quad \text{(3b)–(3d), (3h)–(3j), (14), (15)}. \tag{16}$$

Analogously to Borraz-Sánchez et al. (2016), we now relax this problem by replacing (15a) by inequalities and by dismissing (15b). This leads to the relaxation

$$\min_{x,q,\pi} \sum_{a \in A_{\text{ca}}} c_a x_a \tag{17a}$$

$$\text{s.t.} \quad \text{(3b)–(3d), (3h)–(3j), (14), (15c)}, \tag{17b}$$

$$(\pi_v^d - \pi_u^d) + 2y_a^d(\pi_u^d - \pi_v^d) \ge \Phi_a(|q_a^d|), \quad a = (u,v,\ell) \in A_{\text{ex}}. \tag{17c}$$

Using McCormick inequalities, this relaxation can again be reformulated as a convex MINLP if the potential functions are convex on the nonnegative domain. In addition, for the later considered gas networks, this problem turns into a mixed-integer second-order cone problem. The corresponding reformulations are explicitly outlined in Appendix A. Overall, in Algorithm 1, we can solve Problem (17) w.r.t. the scenario set S at the beginning of each iteration to obtain a lower bound for the objective value of the MINLP (3). Our computational results show that we do not only obtain a tight lower bound, but it is also often the case that the relaxation provides a feasible and, thus, optimal point for the MINLP (3). For more details see Section 6.4.

We finally remark that we also add the obtained lower bounds for the objective value of the MINLP (3) to the described relaxations as well. The important difference is that adding these bounds possibly cut off solutions of the relaxations. However, it will preserve all optimal solutions of the MINLP (3) w.r.t. U in the feasible region of the relaxations. Thus, adding these lower bounds for the objective value can strengthen the presented relaxations.

4.3. **Acyclic Inequalities.** We now briefly review the valid inequalities for potential-based flows derived in Habeck and Pfetsch (2022). Adding these inequalities to the MINLP (3) significantly speeds up the computations. These valid constraints exploit that in the considered setting of potential-based flows, there cannot be any cyclic flow. To see this, let C be a cycle in the undirected version of the network $G = (V, A)$. Considering this cycle in the original directed graph G leads to two subsets of arcs $C_1, C_2 \subseteq A$. Here, C_1 represents the corresponding forward arcs of the cycle and C_2 represents the backward arcs, i.e., those arcs have the opposite direction in the original graph. Summing up the corresponding potential constraints (3e) along the cycle leads to

$$\sum_{a \in C_1} \Phi_a(q_a^d) - \sum_{a \in C_2} \Phi_a(q_a^d) = \sum_{a=(u,v,\ell) \in C_1} \pi_u - \pi_v - \sum_{a=(u,v,\ell) \in C_2} \pi_u - \pi_v = 0.$$

[2]Here, equivalent means in terms of the feasible expansion decisions.

Since the potential functions are strictly increasing and symmetric w.r.t. zero, this implies that there cannot be any cyclic flow. As described in Habeck and Pfetsch (2022), using the flow direction variables y_a^d, this acyclic property can be translated to the valid inequalities

$$\sum_{a \in C_1} y_a^d + \sum_{a \in C_2} (1 - y_a^d) \leq |C| - 1, \quad \sum_{a \in C_1} (1 - y_a^d) + \sum_{a \in C_2} y_a^d \leq |C| - 1. \tag{18}$$

In our computational study, we add these valid inequalities not only to the MINLP (3), but also to the relaxations of the previous section since these relaxations preserve the acyclic property of potential-based flows.

We emphasize that we can add these inequalities for each cycle of the graph that contains all existing arcs and all candidate arcs. This is based on the observation that if such a cycle contains an arc a that is not built, then the corresponding flow is zero and we can arbitrarily choose the flow direction variable y_a^d. Consequently, the corresponding acyclic inequality (18) is redundant.

We also exploit these acyclic inequalities to tighten the given arc flow bounds w.r.t. a given demand vector a priori to solving the relaxations, respectively the MINLP (3). To this end, for each demand vector $d \in S$ and arc $a \in A$, we solve the mixed-integer linear optimization problems

$$\max_{q^d} \quad q_a^d \quad \text{s.t.} \quad (3d), (18), \qquad \min_{q^d} \quad q_a^d \quad \text{s.t.} \quad (3d), (18), \tag{19}$$

to obtain a upper and lower bound for the arc flow q_a^d. We note that Problem (19) is a simple uncapacitated linear flow problem with the additional restriction that the flows are acyclic.

5. How Many Scenarios Do We Need?

We analyze the number of added worst-case scenarios in Algorithm 1 using an academic example. The considered graph appears in similar ways as subnetworks in many real-world utility networks. On the one hand, we show that the considered topology can theoretically lead to many different worst-case scenarios. On the other hand, we highlight that under realistic assumptions on the capacities of the sources, the latter most likely does not occur, which we also empirically observe in our computational study.

We now consider the existing network $G = (V, A)$ with a single source $V_+ = \{u\}$, a single inner node $V_0 = \{0\}$, and the sinks $V_- = \{1, \dots, n\}$ with $n \geq 2$, i.e., $V = V_+ \cup V_- \cup V_0$. The arcs are given by $A = \{(u, 0, \text{ex})\} \cup \{(0, i, \text{ex}) : i \in \{1, \dots, n\}\}$. Here, "ex" represents the label for the existing arcs. For the ease of presentation, we now focus on gas networks, i.e., we consider the potential functions $\Phi_a(q_a) = \Lambda_a q_a |q_a|$. For each arc $a \in A$, we further choose $\Lambda_a = 1$ and for each node $w \in V$, we set the upper and lower potential bounds $[\pi_w^-, \pi_w^+] = [1, 5]$. In addition, we dismiss arc flow bounds. A visualization of this network is given by Figure 1 (A).

We now apply Algorithm 1 to robustify the existing network G. To do so, we have the expansion candidates $A_{\text{ca}} = \{(u, 0, \text{ca})\} \cup \{(0, i, \text{ca}) : i \in \{1, \dots, n\}\}$ with $\Lambda_a = 1, a \in A_{\text{ca}}$, i.e., for each arc, we have an identical expansion arc in parallel to the existing one. Further, we consider the box uncertainty set

$$U = \left\{ d \in \mathbb{R}^V_{\geq 0} : d_u = \sum_{v \in V_-} d_v, \ d_w \in [0, 2], w \in V, \ d_0 = 0 \right\}.$$

For applying Algorithm 1 to this instance, we have to solve in each iteration the adversarial problems (5). Afterward, if applicable, we add the scenario that violates the corresponding potential bounds most.

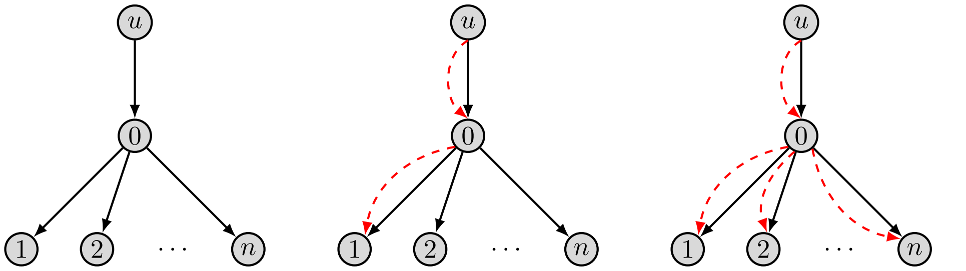

FIGURE 1. Academic network: existing arcs in solid black, expanded arcs in dashed red.

In the first iteration, for one of the node pairs (u, v) with $v \in V_-$, we add the worst-case scenario $d \in U$ given by $d_u = d_v = 2$ and the remaining demands are zero. The corresponding flows q are given by $q_{(u,0)} = q_{(0,v)} = 2$ and the remaining flows are zero. Further, we set the potentials $\pi_u = 8$, $\pi_v = 0$, and the remaining potentials have value 4. We note that these potentials do not have to satisfy any potential bounds in the adversarial problem (5). The point (d, q, π) is a solution of the adversarial problem (5) w.r.t. (u, v) with objective value 8 and, thus, violates the corresponding potential bounds $8 > 4 = 5 - 1 = \pi_u^+ - \pi_v^-$. We note that this potential drop is maximal since for each arc of the unique path from u to v the flow is maximal w.r.t. U and the potential function is strictly increasing. Solving the network expansion MINLP (3) w.r.t. $S = \{d\}$ leads to the expansion decisions $x_{(u,0,\text{ca})} = x_{(0,v,\text{ca})} = 1$, i.e., we expand the capacity along the unique path from u to v; see Figure 1 (B) in which w.l.o.g. $v = 1$ is assumed. In the expanded network, the previous worst-case scenario is now feasible. However, for each other node pair (u, w) with $w \in V_- \setminus \{v\}$, the worst-case scenario with the same structure, i.e., $\tilde{d}_u = \tilde{d}_w = 2$ and the remaining demands are zero, is infeasible. Further, this scenario can again be extended to a solution of the adversarial problem (5) w.r.t. (u, w) in the expanded network and has an objective value of 5, which violates the corresponding potential bounds. Adding this scenario to the worst-case uncertainty set implies that the candidate arc (u, w, ca) has to be built, i.e., $x_{(u,w,\text{ca})} = 1$. Consequently, in the following iterations of Algorithm 1, we add for each node pair (u, w) with $w \in V_-$ the corresponding worst-case scenario with the previously described structure. Thus, Algorithm 1 terminates after n iterations with a robust network, in which every candidate arc is built; see Figure 1 (C). To obtain this robust network, the algorithm considered the described set of demand scenarios

$$S = \{d_u = d_v = 2,\ d_w = 0, w \in V_- \setminus \{v\} \text{ for all } v \in V_-\},$$

which has a cardinality of $|V_-|$. Consequently, the number of worst-case scenarios scales with the number of sinks in the considered network.

However, this relatively large number of scenarios is based on the very small capacity of the source that can only satisfy the maximal demand of a single sink at once. To see this, we now consider an adapted instance in which the capacity of the source suffices to satisfy all demands of the exits at once, i.e., the uncertainty set is given by

$$\tilde{U} = \left\{ d \in \mathbb{R}^V_{\geq 0} : d_u = \sum_{v \in V_-} d_v,\ d_v \in [0, 2], v \in V_-,\ d_0 = 0,\ d_u \leq 2\,|V_-| \right\}.$$

We add another expansion arc $(u, 0, \text{large})$ to A_{ca} with $\Lambda_{(u,0,\text{large})} = 1/(2|V_-| - 1)^2$. This is necessary to guarantee robust feasibility since the maximal arc flow between u and 0 increases within the new uncertainty set $\tilde{U}$, causing a larger potential drop between these nodes. Applying Algorithm 1 to the adapted instance leads to the result that only a single worst-case scenario is necessary to built a robust network. This worst-case scenario is given by $d_u = 2|V_-|$, $d_0 = 0$, and the remaining exits are at their maximum, i.e., $d_v = 2, v \in V_-$. Considering this worst-case scenario leads to the same robust network as in the original instance except that we built the larger arc between u and 0, i.e., we built $(u, 0, \text{large})$ with $\Lambda_{(u,0,\text{large})} = 1/(2|V_-| - 1)^2$ instead of $(u, 0, \text{ca})$ with $\Lambda_{(u,0,\text{ca})} = 1$. Consequently, Algorithm 1 terminates after a single iteration with an optimal solution. More general, for the considered network, it can be shown that the number of worst-case scenarios is bounded from above by $\lceil 2|V_-|/d_u^+ \rceil$, where d_u^+ is the maximal capacity of the single source. This is based on the observation that for robustifying the considered network, for each sink, it suffices that there is at least one scenario in which the demand of the sink is at its maximum. The latter is not necessarily true for general networks. Concluding, the number of worst-case scenarios necessary to obtain a robust network directly depends on the capacity of the single source in the considered network topology.

We emphasize that this topology or related ones with the same behavior regarding the worst-case scenarios are contained as subnetworks in many real-world instances of utility networks. More precisely, the single source corresponds to the connection point to a large distribution network and the remaining network corresponds to a local distribution network. Thus, it is natural that the single source can provide the demand of all exits. For this subnetwork only a single worst-case scenario is then sufficient to guarantee robust feasibility. This illustrates that the approach is especially suitable for real-world utility networks since, most likely, only a few worst-case scenarios are necessary to built a robust network. This is in line with our computational study, in which we only need a few worst-case scenarios and this number of scenarios is often close to the number of different sources in the network.

6. Computational Study

We now apply the presented adversarial approach to gas networks. To this end, we consider different use cases such as robustifying existing networks and building new ones from scratch. In Sections 6.1 and 6.2, we discuss the considered gas network instances and the uncertainty modeling. In the Section 6.3, we then specify the implementation of Algorithm 1 and how we incorporate the enhanced solution techniques of Section 4. Finally, we present and discuss the numerical results in Section 6.4.

6.1. **Gas Networks.** All the instances used in the computational study are based on the GasLib library; see Schmidt et al. (2017). We consider the network GasLib-40 as given in Schmidt et al. (2017). Moreover, we create one larger network based on the significantly larger instance GasLib-135. In continuation of the GasLib notation, we call the newly created instance GasLib-60, i.e., it has 60 nodes. We obtain this network by removing the pipes pipe_46, pipe_93, pipe_96, pipe_103, pipe_104, and pipe_106 from the GasLib-135 network. Then, GasLib-60 represents the weakly connected component containing source_3. The resulting network has 60 nodes, 3 sources, 39 sinks, 61 pipes, and 18 compressors.

For the networks $G = (V, A)$ of GasLib-40 and GasLib-60, we now create different instances as follows. The set V of nodes remains unchanged. Since we consider pipe-only networks, we replace all occurring resistors, control valves, and compressors by so-called short pipes, i.e., by pipes of zero length that do not induce any pressure loss ($\Lambda_a = 0$).

We consider three options on how to choose the existing pipes A_{ex} from the set A, which consists of pipes and short pipes.

In the option unchanged, we set $A_{\text{ex}} = A$, i.e., except for the replaced active elements, the set A_{ex} of existing arcs coincides with the set of arcs of the given GasLib instance. In the option spanning tree, the existing network is assumed to be a spanning tree. Thus, for the given gas network instance, we compute a spanning tree, which also contains all short pipes of the network. The arcs of this spanning tree then represent the existing network, i.e., these arcs are stored in A_{ex}. In the option greenfield, we set $A_{\text{ex}} = \emptyset$, i.e., we assume that no arcs are built yet.

To create the candidate arcs A_{ca}, we apply the following procedure. All short pipes that are already an element of A_{ex} are not considered as possible candidate arcs and the remaining short pipes are added once to the set of candidate arcs A_{ca}. For each pipe of the original network $G = (V, A)$, we then add multiple candidate arcs in parallel with different choices for the corresponding diameter. To do so, we introduce factors $\tau_1, \dots, \tau_m \in (0, \infty)$ with $m \geq 1$ and then each pipe is added m times with the reported diameter of the GasLib multiplied once by τ_i with $i \in \{1, \dots, m\}$. For the instances unchanged and spanning tree, we consider the factors $\{0.3, 0.7, 1.0, 1.3\}$, i.e., for each expansion candidate, we have four diameter options. For the even more challenging greenfield instances, we choose three diameter options per expansion candidate given by the factors $\{0.5, 1.0, 1.5\}$.

For estimating the investment costs of building new pipes, we follow the cost estimation of Mischner et al. (2015) and Reuß et al. (2019). Consequently, the costs of building a pipe a (in €/m, i.e., per length) depend on the corresponding diameter D_a (in mm). These investment costs are computed using $278.24 \exp(1.6 D_a)$. We further do not charge any costs for building short pipes.

We now briefly discuss the implementation of the potential-based flow model for the considered case of gas networks. For an arc $a \in A_{\text{ex}} \cup A_{\text{ca}}$, the potential function is explicitly given by $\Phi_a(q_a) = \Lambda_a q_a |q_a|$; see Gross et al. (2019). The pressure loss coefficient $\Lambda_a \geq 0$ is computed using the formula

$$\Lambda_a = \left(\frac{4}{\pi}\right)^2 \lambda_a \frac{R_{\text{s}} T_{\text{m}} L_a z_{\text{m},a}}{D_a^5}$$

with λ_a being the pipe's friction factor given by the formula of Nikuradse, R_{s} the specific gas constant, T_{m} a constant mean temperature, L_a the pipe's length, and D_a the pipe's diameter. In addition, $z_{\text{m},a}$ is the pipe's mean compressibility factor given by the formula of Papay and an a priori estimation of the mean pressure. Furthermore, we set $\Lambda_a = 0$ if a is a short pipe. For more information and detailed explanations, we refer to Fügenschuh et al. (2015).

6.2. **Uncertainty Modeling.** In the computational study, we consider four different polyhedral uncertainty sets. We start with a baseline scenario $d^{\text{base}} \in \mathbb{R}^V_{\geq 0}$, which then is affected by certain demand fluctuations. For GasLib-40, we choose the scenario reported in Schmidt et al. (2017) as the baseline scenario. For the newly created instance GasLib-60, we choose the following baseline scenario. The demand is set to $520\,(1000\,\text{Nm}^3/\text{h})$ for all sources and to $40\,(1000\,\text{Nm}^3/\text{h})$ for all sinks.

As introduced in Equation (2), each uncertainty set consists of all balanced demands

$$L := \left\{ d \in \mathbb{R}^V_{\geq 0} : \sum_{u \in V_+} d_u = \sum_{u \in V_-} d_u, \ d_u = 0, \ u \in V_0 \right\}$$

intersected with a non-empty and compact set $Z \subset \mathbb{R}^V$. We now discuss our polyhedral choices for this compact set Z.

TABLE 1. Parameterization of the uncertainty sets.

$\underline{z}^-$	$\bar{z}^-$	$\underline{z}^+$	$\bar{z}^+$	$\underline{i}$	$\bar{i}$	$\bar{d}$	w
0.6	1.4	0.7	1.3	0.8	1.2	0.1	80

We start with a simple box as a first uncertainty set, i.e., lower and upper bounds for the injections and withdrawals are additionally imposed. For the sinks, we consider a lower bound $\underline{z}^- \in [0,1]$ and an upper bound $\bar{z}^- \in [1,\infty)$, which indicate the percentage deviation from the baseline scenario. Analogously, for the sources, we define a lower bound $\underline{z}^+ \in [0,1]$ and an upper bound $\bar{z}^+ \in [1,\infty)$. Then, the box uncertainty set is given by

$$U_{\text{box}} := \left\{ d \in L : d_u \in [\underline{z}^- d_u^{\text{base}}, \bar{z}^- d_u^{\text{base}}],\ u \in V_-,\ d_u \in [\underline{z}^+ d_u^{\text{base}}, \bar{z}^+ d_u^{\text{base}}],\ u \in V_+ \right\}.$$

For $\underline{z}^- = \underline{z}^+ = 0$, this uncertainty set allows that sinks or sources fail completely, i.e., they are switched off.

Based on this box uncertainty set, we define three further uncertainty sets. For the first modification, we ensure by two additional inequalities that the total amount of injections does not exceed or drop below a certain level regarding the total injections in the baseline scenario. Hence, we introduce a percentage bound for the lower ($\underline{i} \in [0,1]$) and upper ($\bar{i} \in [1,\infty)$) level of total injections. Then, the box uncertainty set with additional bounds on the total injections is given by

$$U_{\text{sum}} := U_{\text{box}} \cap \left\{ d \in L : \underline{i} \sum_{u \in V_+} d_u^{\text{base}} \le \sum_{u \in V_+} d_u \le \bar{i} \sum_{u \in V_+} d_u^{\text{base}} \right\}.$$

For the next modification of the box uncertainty set U_{box}, we bound the absolute difference of deviations from the baseline scenario for selected pairs of withdrawals. To do so, we consider a randomly chosen subset of the sinks $\tilde{V}_- \subset V_-$ and an upper bound for the absolute difference $\bar{d} \ge 0$. Then, for a balanced demand $d \in L$, we add the inequality

$$\left|(d_u^{\text{base}})^{-1} d_u - (d_v^{\text{base}})^{-1} d_v\right| \le \bar{d}, \quad (u,v) \in \tilde{V}_- \times \tilde{V}_-. \tag{20}$$

This leads to the third uncertainty set

$$U_{\text{corr}} := U_{\text{box}} \cap \{d \in L : (20) \text{ holds}\}.$$

Before we continue with the fourth uncertainty set, let us discuss some details about Condition (20) and its implementation. The idea behind this condition is that there could be withdrawals that follow the same consumption pattern, e.g., due to temperature dependency in case of an energy carrier used for heating. In our computational study, we obtain the set $\tilde{V}_-$ in (20) by randomly selecting sinks from V_- until a certain percentage w of the number of sinks is reached or just exceeded. The selected sinks form the set $\tilde{V}_-$.

The fourth uncertainty set is the intersection of all three previously defined uncertainty sets. Thus, it is given by

$$U_{\text{all}} := U_{\text{box}} \cap U_{\text{sum}} \cap U_{\text{corr}}.$$

Table 1 provides an overview of the specific parameterization of the uncertainty sets used. We consider the case that the demand of sinks fluctuates slightly more than the demand of sources, i.e., $[\underline{z}^+, \bar{z}^+] \subset [\underline{z}^-, \bar{z}^-]$ holds. Moreover, in case of correlated demands, i.e., U_{corr} and U_{all}, we assume that not all but 80 % of the sinks are correlated.

6.3. **Algorithmic and Computational Setup.** We now briefly discuss the implementation of the enhanced solution techniques of Section 4 in Algorithm 1. More precisely, we consider two different configurations of this algorithm in the following. For both approaches, we model the MINLP for the expansion decision with flow direction variables, i.e., we use Model (16). Analogously, we also model the adversarial problems (5) with flow direction variables, which we outline in Appendix A. For doing so, we use a single flow direction variable for parallel pipes because parallel pipes always have the same flow direction. Further, we require by additional constraints that only a single expansion pipe can be built in parallel to an existing one. This is legitimate because building multiple new parallel pipes can be equivalently reformulated as building a single pipe; see Lenz and Schwarz (2016). Based on preliminary computational results, we add the acyclic inequalities, see Section 4.3, to the occurring MINLPs and also to the convex relaxations (17). As explained in Section 4.2, we further use the optimal objective value of the expansion decision of the previous iteration as a lower bound for the objective value of the MINLPs (16) and the upcoming relaxations Reduced Relaxation as well as Problems (17). The considered pipe-only gas networks typically do not impose any bounds on the arc flow because the flow is implicitly bounded by the potential bounds at the incident nodes. Consequently, we can dismiss the very large flow bounds of the GasLib instances and we do not have to solve the adversarial problems (6) and (7). However, prior to each iteration, we apply some basic presolve to compute tighter lower and upper arc flow bounds by solving Problems (19) in order to strengthen the formulations. We note that all instances satisfy the requirements of Lemma 3 and, thus, we check robust feasibility using the characterization of this lemma. Finally, for both approaches, the scenario set S only contains the baseline scenario d^{base} in the first iteration, i.e., we set $S = \{d^{\text{base}}\}$.

After these adaptions, we denote as the baseline approach (MINLP_Acyclic) the plain version of Algorithm 1. For the second approach (Reduced_Convex), we extend this baseline approach by two methods to compute tighter lower bounds for the optimal objective value of the robust network design problem (16), which are computed iteratively. More precisely, before solving the expansion problem, i.e., before Line 2 in Algorithm 1, we first solve the relaxation Reduced Relaxation (except for the first iteration), i.e., we solve the expansion problem only w.r.t. the last added scenario; see Section 4.2. Second, we solve the mixed-integer convex relaxation (17) w.r.t. S, i.e., we consider all found worst-case scenarios. After solving each of these relaxations, we check if the obtained solution is feasible for the network design problem (16) by solving the latter with fixed expansion decisions. If this is the case, we directly go to Line 4 of Algorithm 1 and check robust feasibility of the obtained network design. If applicable, we also update the best known lower bound that we add to the upcoming MINLPs or convex relaxations to bound the objective value from below. The main intuition behind the approach Reduced_Convex consists of avoiding to solve the challenging MINLP (16), whose size increases from iteration to iteration, by solving an MINLP of "fixed" size (Reduced Relaxation) or a mixed-integer second-order cone problem (17).

We finally note that the models are implemented in Python 3.7 with Pyomo 6.7.0 (Bynum et al. (2021)) and we solve the models using Gurobi 10.0.3 (Gurobi Optimization, LLC (2022)). The computations are carried out on a single node of a server[3] with Intel XEON SP 6126 CPUs. Further, we set a memory limit of 64 GB, a total time limit of 24 h, and limit the number of threads to 4. Additionally, we use the Python package perprof-py (Soares Siqueira et al. (2016)) to produce the performance profiles as described in Dolan and Moré (2002).

[3] https://elwe.rhrk.uni-kl.de/elwetritsch/hardware.shtml

TABLE 2. Runtimes and number of adversarial scenarios of the approach MINLP_Acyclic. Left: Instances w.r.t. unchanged GasLib-40. Right: Instances w.r.t. unchanged GasLib-60.

#Solved	4 of 4		
	Min	Median	Max
#Iterations	2	3	3
#Scenarios	1	2	2
Runtime (s)	807.65	1395.33	1578.68

#Solved	4 of 4		
	Min	Median	Max
#Iterations	2	2	2
#Scenarios	1	1	1
Runtime (s)	1117.37	1175.83	3009.57

TABLE 3. Runtimes and number of adversarial scenarios of the approach Reduced_Convex. Left: Instances w.r.t. unchanged GasLib-40. Right: Instances w.r.t. unchanged GasLib-60.

#Solved	4 of 4		
	Min	Median	Max
#Iterations	2	3	3
#Scenarios	1	2	2
Runtime (s)	332.21	1149.98	2042.90

#Solved	4 of 4		
	Min	Median	Max
#Iterations	2	2	2
#Scenarios	1	1	1
Runtime (s)	564.06	995.62	1037.74

6.4. **Numerical Results.** We now apply the two presented variants MINLP_Acyclic and Reduced_Convex of Algorithm 1 to the gas network instances described in Section 6.1 and the uncertainty sets described in Section 6.2. Consequently, for each network, we obtain four different instances. For most of the instances checking robust feasibility, i.e., solving the adversarial problems, only has a moderate contribution to the overall runtimes. Relative to the runtimes of the algorithm, the total time spent to solve the adversarial problems (10), which are MILPs, is below 1.3 %. For the more challenging nonlinear adversarial problems (5), the median of the aggregated runtimes relative to the runtimes of the algorithm is below 12.5 %. Only in some cases this percentage increases to at most 88.26 %, which is often the case if the algorithm only needs two or less iterations. For obtaining these moderate runtimes regarding the aggregated runtimes of the adversarial problems, Lemma 3 is key. In particular, the approach benefits from the property that utility networks typically contain a small number of sources, e.g., the considered instances contain 3 sources. Since the runtimes of the adversarial problems are moderate compared to the total runtimes of the algorithm in most cases, we only focus on the total runtimes of Algorithm 1 in the following.

6.4.1. *Robustifying Existing Networks.* We start by applying our approach to robustify the existing gas networks GasLib-40 and GasLib-60 by building new pipes in parallel to existing ones. In this case, the majority of pipes is already existing and we selectively expand the capacity of the network to resolve bottlenecks and to guarantee robust feasibility. In Table 2, we summarize the statistics of the total runtimes and the number of added adversarial scenarios for the plain version of Algorithm 1, i.e., for the variant MINLP_Acyclic. Analogously, we summarize the statistics for the variant Reduced_Convex in Table 3. For these instances at most two adversarial scenarios are sufficient to compute a robust network. We emphasize that this small number of adversarial scenarios can be most likely traced back to the typical structure of gas networks that a small number of sources can supply the majority of sinks. This usually leads to a small number of worst-case scenarios as illustrated in Section 5. Regarding the runtimes, the variant Reduced_Convex is slightly faster on the majority of instances but not on every instance. This can be

TABLE 4. Runtimes and number of adversarial scenarios of the approach MINLP_Acyclic. Left: Instances w.r.t. spanning tree GasLib-40. Right: Instances w.r.t. spanning tree GasLib-60.

#Solved	4 of 4		
	Min	Median	Max
#Iterations	2	2	2
#Scenarios	1	1	1
Runtime (s)	951.95	6281.03	7818.14

#Solved	4 of 4		
	Min	Median	Max
#Iterations	2	3	3
#Scenarios	1	2	2
Runtime (s)	274.42	1743.79	2875.57

TABLE 5. Runtimes and number of adversarial scenarios of the approach Reduced_Convex. Left: Instances w.r.t. spanning tree GasLib-40. Right: Instances w.r.t. spanning tree GasLib-60.

#Solved	4 of 4		
	Min	Median	Max
#Iterations	2	2	2
#Scenarios	1	1	1
Runtime (s)	312.49	576.27	726.63

#Solved	4 of 4		
	Min	Median	Max
#Iterations	2	3	3
#Scenarios	1	2	2
Runtime (s)	215.01	805.01	1954.97

explained by the observation that in the approach Reduced_Convex all of the expansion MINLPs (16) could be solved by the relaxations, i.e., by either the Reduced Relaxation or the mixed-integer second-order cone relaxation (17). We note that this is not the case in general and also does not hold for the following instances. Overall, both variants of Algorithm 1 are very effective to robustify existing gas networks.

6.4.2. *Extending Backbone Networks.* We now consider the case that a spanning tree is given as the existing network and we expand this network by new pipes, which are not necessarily in parallel to the existing ones. We summarize the statistics of the considered approaches in Tables 4 and 5. As before the number of adversarial scenarios is very low, which can be explained as in the previous section. Regarding the runtimes, the approach Reduced_Convex significantly outperforms the plain version of Algorithm 1. For the GasLib-40, this can again be explained by the fact that all occurring MINLPs could be solved by the relaxations. This is not the case for all instances of GasLib-60. However, the majority of the obtained lower bounds for the optimal objective value of the corresponding MINLP is close to the optimal value. More precisely, the mixed-integer second-order cone relaxation (17) solves the MINLP 5 out of 7 times. Further, the gap[4] between the optimal objective value of the relaxation and the one of the corresponding MINLP is at most 0.85 %. Additionally, the Reduced Relaxation solves 4 out of 7 times the MINLP to optimality and the maximal gap is 25 %. Thus, for the considered instances, solving additional relaxations significantly speeds up the solution process. Overall, the approach Reduced_Convex is to be preferred to extend existing networks in a robust way.

6.4.3. *Greenfield Approach.* We finally turn to the greenfield approach in which we design a network from scratch. As expected this setup is significantly more challenging than the previous ones, which is also reflected in the computational results. As outlined in Table 6, the plain version of Algorithm 1 can only solve a single instance for the GasLib-40 and a single one for the GasLib-60 network. Applying the enhanced variant Reduced_Convex significantly improves the performance. In particular, it can solve 3 out of 4 instances

[4]We compute the gap as proposed by CPLEX under https://www.ibm.com/docs/en/icos/22.1.1?topic=parameters-relative-mip-gap-tolerance.

TABLE 6. Runtimes and number of adversarial scenarios of the approach MINLP_Acyclic. Left: Instances w.r.t. greenfield GasLib-40. Right: Instances w.r.t. greenfield GasLib-60.

#Solved	1 of 4		
	Min	Median	Max
#Iterations	2	2	2
#Scenarios	1	1	1
Runtime (s)	7320.85	7320.85	7320.85

#Solved	1 of 4		
	Min	Median	Max
#Iterations	3	3	3
#Scenarios	2	2	2
Runtime (s)	81 895.84	81 895.84	81 895.84

TABLE 7. Runtimes and number of adversarial scenarios of the approach Reduced_Convex. Left: Instances w.r.t. greenfield GasLib-40. Right: Instances w.r.t. greenfield GasLib-60.

#Solved	3 of 4		
	Min	Median	Max
#Iterations	2	4	4
#Scenarios	1	3	3
Runtime (s)	4066.79	39 963.87	50 183.53

#Solved	1 of 4		
	Min	Median	Max
#Iterations	3	3	3
#Scenarios	2	2	2
Runtime (s)	51 290.35	51 290.35	51 290.35

for the GasLib-40 and a single one for the GasLib-60; see Table 7. Compared to the previous cases, one can observe that slightly more adversarial scenarios are necessary to build a robust network from scratch. However, the approach still requires only a moderate amount of worst-case scenarios. We note that the number of computed adversarial scenarios matches the number of sources of the network, which is in line with the explanations provided in Section 5. The improved performance w.r.t. the runtimes of the approach Reduced_Convex can again be explained by tight gaps w.r.t. the objective values of the relaxations and the corresponding MINLPs. More precisely, the Reduced Relaxation solves the MINLP 4 out of 9 times and the gap is at most 1.65 %. The mixed-integer second-order code relaxation (17) solves the MINLP 9 out of 9 times. The good performance w.r.t. the gap between the optimal objective value of the mixed-integer convex relaxation (17) and the MINLP (16) is in line with the computational results of Borraz-Sánchez et al. (2016). However, we note that the runtimes for the relaxation (17) and the MINLP (16) drastically increase from iteration to iteration. For the unsolved instances, this results in reaching the time limit of 24 h. In these cases, for the MINLPs and the mixed-integer convex relaxations (17), it seems to be the case that proving optimality is the biggest challenge for the solvers during the solution process. Thus, both approaches cannot solve all instances within the set time limit if designing a network from scratch.

Overall, our computational study based on real-world instances reveals two main insights. (i) For the considered instances, only a moderate number of worst-case scenarios is necessary to compute a robust network design, which makes the presented approach very effective in practice. (ii) The variant Reduced_Convex significantly outperforms the plain version of Algorithm 1. Thus, for most of the instances, it is worth solving additional relaxations to provide lower bounds for the objective value of the challenging MINLPs, which then speed up the overall solution process. We finally highlight this effect by the performance profile in Figure 2.

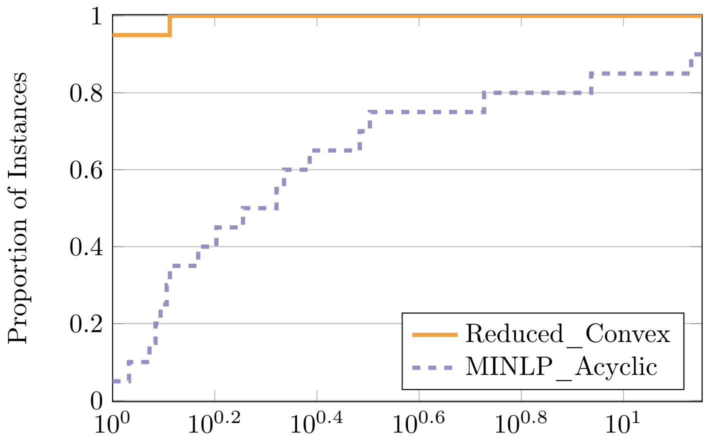

Figure 2. Performance profile for the runtimes regarding all instances that are solved by at least one approach.

7. Conclusion

We studied an adjustable robust mixed-integer nonlinear network design problem with demand uncertainties. To this end, we considered nonlinear potential-based flows, which allow to model different types of utility networks such as gas, hydrogen, or water networks. For the considered problem, we developed an exact adversarial approach that exploits the structural properties of the network and flows to obtain a robust network design that is protected from demand uncertainties. Finally, we demonstrated the applicability of the developed approach using the example of realistic gas networks instances. The computational results highlight that for these instances only a very small number of worst-case scenarios is necessary to obtain a robust network, which makes the presented approach very efficient in practice.

One promising direction for future research consists of developing valid inequalities for network expansion problems with nonlinear potential-based flows. In contrast to the large literature on valid inequalities for network design problems with capacitated linear flows, the corresponding literature on potential-based flows is rather scarce.

Acknowledgements

The authors thank the Deutsche Forschungsgemeinschaft for their support within project B08 in the Sonderforschungsbereich/Transregio 154 "Mathematical Modelling, Simulation and Optimization using the Example of Gas Networks". The computations were executed on the high performance cluster "Elwetritsch" at the TU Kaiserslautern, which is part of the "Alliance of High Performance Computing Rheinland-Pfalz" (AHRP). We kindly acknowledge the support of RHRK.

References

Atamtürk, A. and M. Zhang (2007). "Two-stage robust network flow and design under demand uncertainty." In: *Operations Research* 55.4, pp. 662–673. doi: 10.1287/opre.1070.0428.

Ayoub, J. and M. Poss (2016). "Decomposition for adjustable robust linear optimization subject to uncertainty polytope." In: *Computational Management Science* 13.2, pp. 219–239. doi: 10.1007/s10287-016-0249-2.

Aßmann, D., F. Liers, and M. Stingl (2019). "Decomposable robust two-stage optimization: An application to gas network operations under uncertainty." In: *Networks* 74.1, pp. 40–61. DOI: 10.1002/net.21871.

Ben-Ameur, W. and H. Kerivin (2005). "Routing of uncertain traffic demands." In: *Optimization and Engineering* 6.3, pp. 283–313. DOI: 10.1007/s11081-005-1741-7.

Bertsimas, D., R. Cory-Wright, J. Pauphilet, and P. Petridis (2023). *A Stochastic Benders Decomposition Scheme for Large-Scale Data-Driven Network Design*. Tech. rep. URL: https://arxiv.org/abs/2303.07695.

Bertsimas, D., I. Dunning, and M. Lubin (2016). "Reformulation versus cutting-planes for robust optimization: A computational study." In: *Computational Management Science* 13.2, pp. 195–217. DOI: 10.1007/s10287-015-0236-z.

Bienstock, D. and N. Özbay (2008). "Computing robust basestock levels." In: *Discrete Optimization* 5.2, pp. 389–414. DOI: 10.1016/j.disopt.2006.12.002.

Borraz-Sánchez, C., R. Bent, S. Backhaus, H. Hijazi, and P. Van Hentenryck (2016). "Convex relaxations for gas expansion planning." In: *INFORMS Journal on Computing* 28.4, pp. 645–656. DOI: 10.1287/ijoc.2016.0697.

Bynum, M. L., G. A. Hackebeil, W. E. Hart, C. D. Laird, B. L. Nicholson, J. D. Siirola, J.-P. Watson, and D. L. Woodruff (2021). *Pyomo–optimization modeling in Python*. Vol. 67. Springer Science & Business Media. DOI: 10.1007/978-3-030-68928-5.

Cacchiani, V., M. Jünger, F. Liers, A. Lodi, and D. R. Schmidt (2016). "Single-commodity robust network design with finite and hose demand sets." In: *Mathematical Programming* 157.1, pp. 297–342. DOI: 10.1007/s10107-016-0991-9.

D'Ambrosio, C., A. Lodi, S. Wiese, and C. Bragalli (2015). "Mathematical programming techniques in water network optimization." In: *European Journal of Operational Research* 243.3, pp. 774–788. DOI: 10.1016/j.ejor.2014.12.039.

Dolan, E. D. and J. J. Moré (Jan. 2002). "Benchmarking optimization software with performance profiles." In: *Mathematical Programming* 91.2, 201–213. DOI: 10.1007/s101070100263.

Fügenschuh, A., B. Geißler, R. Gollmer, A. Morsi, M. E. Pfetsch, J. Rövekamp, M. Schmidt, K. Spreckelsen, and M. C. Steinbach (2015). "Chapter 2: Physical and technical fundamentals of gas networks." In: *Evaluating Gas Network Capacities*, pp. 17–43. DOI: 10.1137/1.9781611973693.ch2.

Gross, M., M. E. Pfetsch, L. Schewe, M. Schmidt, and M. Skutella (2019). "Algorithmic results for potential-based flows: Easy and hard cases." In: *Networks* 73.3, pp. 306–324. DOI: 10.1002/net.21865.

Gurobi Optimization, LLC (2022). *Gurobi Optimizer Reference Manual*. URL: https://www.gurobi.com.

Habeck, O. and M. E. Pfetsch (2022). "Combinatorial acyclicity models for potential-based flows." In: *Networks* 79.1, pp. 83–104. DOI: 10.1002/net.22038.

Humpola, J. and A. Fügenschuh (2015). "Convex reformulations for solving a nonlinear network design problem." In: *Computational Optimization and Applications* 62.3, pp. 717–759. DOI: 10.1007/s10589-015-9756-2.

Humpola, J., A. Fügenschuh, T. Lehmann, R. Lenz, R. Schwarz, and J. Schweiger (2015). "Chapter 7: The specialized MINLP approach." In: *Evaluating Gas Network Capacities*, pp. 123–143. DOI: 10.1137/1.9781611973693.ch7.

Klimm, M., M. E. Pfetsch, R. Raber, and M. Skutella (2023). "On the robustness of potential-based flow networks." In: *Mathematical Programming* 197.1, pp. 337–374. DOI: 10.1007/s10107-021-01760-w.

Koster, A. M. C. A., M. Kutschka, and C. Raack (2013). "Robust network design: formulations, valid inequalities, and computations." In: *Networks* 61.2, pp. 128–149. DOI: 10.1002/net.21497.

Kuchlbauer, M., F. Liers, and M. Stingl (2022). "Adaptive bundle methods for nonlinear robust optimization." In: *INFORMS Journal on Computing* 34.4, pp. 2106–2124. DOI: 10.1287/ijoc.2021.1122.

Labbé, M., F. Plein, and M. Schmidt (2020). "Bookings in the European gas market: characterisation of feasibility and computational complexity results." In: *Optimization and Engineering* 21.1, pp. 305–334. DOI: 10.1007/s11081-019-09447-0.

Lefebvre, H., M. Schmidt, and J. Thürauf (2022). *Using Column Generation in Column-and-Constraint Generation for Adjustable Robust Optimization.* Tech. rep. URL: https://optimization-online.org/2023/10/using-column-generation-in-column-and-constraint-generation-for-adjustable-robust-optimization/.

Lenz, R. and R. Schwarz (2016). *Optimal Looping of Pipelines in Gas Networks.* Tech. rep. ZIB Report (16-67): Zuse Institut Berlin. URL: https://opus4.kobv.de/opus4-zib/frontdoor/index/index/docId/6156.

Li, Y., S. S. Dey, and N. V. Sahinidis (2024). *A reformulation-enumeration MINLP algorithm for gas network design.* Tech. rep. URL: https://arxiv.org/abs/2307.07648.

McCormick, G. P. (1976). "Computability of global solutions to factorable nonconvex programs. I. Convex underestimating problems." In: *Mathematical Programming* 10.2, pp. 147–175. DOI: 10.1007/BF01580665.

Mischner, J., H. Fasold, and J. Heymer (2015). *gas2energy.net: Systemplanerische Grundlagen der Gasversorgung.* Edition GWF. Gas, Erdgas. Division Deutscher Industrieverlag GmbH.

Pfetsch, M. E. and A. Schmitt (2023). "A generic optimization framework for resilient systems." In: *Optimization Methods & Software* 38.2, pp. 356–385. DOI: 10.1080/10556788.2022.2142581.

Poss, M. and C. Raack (2013). "Affine recourse for the robust network design problem: between static and dynamic routing." In: *Networks* 61.2, pp. 180–198. DOI: 10.1002/net.21482.

Raghunathan, A. U. (2013). "Global Optimization of Nonlinear Network Design." In: *SIAM Journal on Optimization* 23.1, pp. 268–295. DOI: 10.1137/110827387.

Reuß, M., L. Welder, J. Thürauf, J. Linßen, T. Grube, L. Schewe, M. Schmidt, D. Stolten, and M. Robinius (2019). "Modeling hydrogen networks for future energy systems: A comparison of linear and nonlinear approaches." In: *International Journal of Hydrogen Energy* 44.60, pp. 32136 –32150. DOI: 10.1016/j.ijhydene.2019.10.080.

Robinius, M., L. Schewe, M. Schmidt, D. Stolten, J. Thürauf, and L. Welder (2019). "Robust optimal discrete arc sizing for tree-shaped potential networks." In: *Computational Optimization and Applications* 73.3, pp. 791–819. DOI: 10.1007/s10589-019-00085-x.

Santoso, T., S. Ahmed, M. Goetschalckx, and A. Shapiro (2005). "A stochastic programming approach for supply chain network design under uncertainty." In: *European Journal of Operational Research* 167.1, pp. 96–115. DOI: 10.1016/j.ejor.2004.01.046.

Schmidt, M., D. Aßmann, R. Burlacu, J. Humpola, I. Joormann, N. Kanelakis, T. Koch, D. Oucherif, M. E. Pfetsch, L. Schewe, R. Schwarz, and M. Sirvent (2017). "GasLib—A Library of Gas Network Instances." In: *Data* 2.4. DOI: 10.3390/data2040040.

Schmidt, M. and J. Thürauf (2022). *An Exact Method for Nonlinear Network Flow Interdiction Problems.* Tech. rep. URL: https://optimization-online.org/2022/10/an-exact-method-for-nonlinear-network-flow-interdiction-problems/.

Soares Siqueira, A., R. G. Costa da Silva, and L.-R. Santos (2016). "Perprof-py: A Python Package for Performance Profile of Mathematical Optimization Software." In: *Journal of Open Research Software* 4.1, p. 12. DOI: 10.5334/jors.81.

Sundar, K., S. Misra, A. Zlotnik, and R. Bent (2021). "Robust Gas Pipeline Network Expansion Planning to Support Power System Reliability." In: *2021 American Control Conference (ACC)*, pp. 620–627. DOI: 10.23919/ACC50511.2021.9483249.

Takeda, A., S. Taguchi, and R. H. Tütüncü (2008). "Adjustable Robust Optimization Models for a Nonlinear Two-Period System." In: *Journal of Optimization Theory and Applications* 136.2, pp. 275–295. DOI: 10.1007/s10957-007-9288-8.

Thürauf, J. (2022). "Deciding the feasibility of a booking in the European gas market is coNP-hard." In: *Annals of Operations Research* 318.1. DOI: 10.1007/s10479-022-04732-1.

Yanıkoğlu, I., B. L. Gorissen, and D. den Hertog (2019). "A survey of adjustable robust optimization." In: *European Journal of Operational Research* 277.3, pp. 799–813. DOI: 10.1016/j.ejor.2018.08.031.

Zhao, L. and B. Zeng (2012). *An Exact Algorithm for Two-stage Robust Optimization with Mixed Integer Recourse Problems.* Tech. rep. URL: https://optimization-online.org/2012/01/3310/.

Appendix A. Linearization of Bilinear Terms

We now derive an exact reformulation of the bilinear terms in the left-hand sides of Constraints (15) using McCormick inequalities. To do so, for each arc $a = (u, v, \ell)$, we linearize the term $2y_a^d(\pi_u^d - \pi_v^d)$ by introducing the additional variable $\gamma_a^d \in \mathbb{R}$ and the four inequalities

$$2(\pi_u^d - \pi_v^d) - 2(1 - y_a^d)(\pi_u^+ - \pi_v^-) \leq \gamma_a^d, \tag{21a}$$
$$2(\pi_u^d - \pi_v^d) - 2(1 - y_a^d)(\pi_u^- - \pi_v^+) \geq \gamma_a^d, \tag{21b}$$
$$2y_a^d(\pi_u^- - \pi_v^+) \leq \gamma_a^d, \tag{21c}$$
$$2y_a^d(\pi_u^+ - \pi_v^-) \geq \gamma_a^d. \tag{21d}$$

If $y_a^d = 1$ holds, then from Constraints (21a) and (21b), it follows $\gamma_a^d = 2(\pi_u^d - \pi_v^d)$. Further, every potential vector $\pi \in \mathbb{R}^V$ that satisfies the potential bounds (3j) also satisfies together with γ_a^d the Constraints (21c) and (21d). If $y_a^d = 0$ holds, then from Constraints (21c) and (21d), it follows $\gamma_a^d = 0$. Further, every potential vector $\pi \in \mathbb{R}^V$ that satisfies the potential bounds (3j), then also satisfies together with γ_a^d the Constraints (21a) and (21b). Thus, for every vector $(\pi_u^d, \pi_v^d, \gamma_a^d)$ that satisfies (21), it holds $\gamma_a^d = 2y_a^d(\pi_u^d - \pi_v^d)$.

Using the previous linearization, we can replace the bilinear terms in the left-hand sides of (15) by γ_a^d. Consequently, Constraints (21) together with the constraints

$$(\pi_v^d - \pi_u^d) + \gamma_a^d = \Phi_a(|q_a^d|), \quad a = (u, v, \ell) \in A_{\text{ex}}, \tag{22a}$$
$$(\pi_v^d - \pi_u^d) + \gamma_a^d \leq \Phi_a(|q_a^d|) + (1 - x_a)M_a^+, \quad a = (u, v, \ell) \in A_{\text{ca}}, \tag{22b}$$
$$(\pi_v^d - \pi_u^d) + \gamma_a^d \geq \Phi_a(|q_a^d|) + (1 - x_a)M_a^-, \quad a = (u, v, \ell) \in A_{\text{ca}}, \tag{22c}$$

leads to an equivalent reformulation of the Constraints (15).

Analogously, we can linearize the bilinear terms in the Relaxation (17). This then leads to a mixed-integer second-order cone problem for the considered case of gas networks, in which the potential function satisfies $\Phi_a(|q_a|) = \Lambda_a q_a^2$.

We finally discuss that we can use the previous linearization (21) and (22) with minor adaptions to model the adversarial problems (5)–(7) as MINLPs. Since the adversarial problems do not contain lower or upper potential bounds, we have to replace these potential bounds in Constraints (21a)–(21d) by valid bounds so that the optimal value of an optimal solution to the adversarial problems (5)–(7) is not changed. To this end, for each arc $a \in A$, we can compute a lower and upper arc flow bound w.r.t. the uncertainty set by solving the optimization problems

$$\max_{q^d, d} \quad q_a^d \quad \text{s.t.} \quad (3d),\ (18),\ d \in U, \qquad \min_{q^d, d} \quad q_a^d \quad \text{s.t.} \quad (3d),\ (18),\ d \in U.$$

Similar to Problem (19), these problems compute upper and lower arc flow bounds by solving an uncapacitated linear flow model with the additional restriction of acyclic flows over the given demand uncertainty set. We now denote a corresponding bound on the maximum absolute arc flow of a by $\tilde{q}_a$. From this, we obtain the inequalities $-\Lambda_a \tilde{q}_a^2 \leq \pi_u^d - \pi_v^d \leq \Lambda_a \tilde{q}_a^2$, which are valid for all feasible points of the adversarial problems (5)–(7). Consequently, for applying the McCormick inequalities and model the adversarial problems (5)–(7) as MINLPs, we replace in the above linearization the Constraints (21a)–(21d) by

$$2(\pi_u^d - \pi_v^d) - 2(1 - y_a^d)\Lambda_a \tilde{q}_a^2 \leq \gamma_a^d, \quad 2(\pi_u^d - \pi_v^d) + 2(1 - y_a^d)\Lambda_a \tilde{q}_a^2 \geq \gamma_a^d,$$
$$-2y_a^d \Lambda_a \tilde{q}_a^2 \leq \gamma_a^d, \quad 2y_a^d \Lambda_a \tilde{q}_a^2 \geq \gamma_a^d.$$

We note that for this linearization, we can use any bound $\tilde{q}_a$ on the absolute flow. Finally, we can fix the potential level of an arbitrary node in the adversarial problems (5)–(7) due to Lemma 1.

(J. Thürauf, M. Schmidt) Trier University, Department of Mathematics, Universitätsring 15, 54296 Trier, Germany

(J. Grübel) University of Technology Nuremberg (UTN), Department Liberal Arts and Sciences, Ulmenstrasse 52h, 90443 Nuremberg, Germany

Email address: johannes.thuerauf@uni-trier.de

Email address: julia.gruebel@utn.de

Email address: martin.schmidt@uni-trier.de